P2mit

NASA TECHNICAL NOTE **NASA TN D-7513**

FILM COOLING IN A COMBUSTOR OPERATING AT FUEL-RICH EXIT CONDITIONS

by Robert R. Tacina and Cecil J. Marek

Lewis Research Center

Cleveland, Ohio 44135

NATIONAL AERONAUTICS AND SPACE ADMINISTRATION • WASHINGTON, D. C. • JANUARY 1974

1. Report No. NASA TN D-7513	2. Government Accession No.	3. Recipient's Catalog No.
4. Title and Subtitle FILM COOLING IN A COMBUSTOR OPERATING AT FUEL-RICH EXIT CONDITIONS		5. Report Date January 1974 6. Performing Organization Code
7. Author(s) by Robert R. Tacina and Cecil J. Marek		8. Performing Organization Report No. E-7561
9. Performing Organization Name and Address Lewis Research Center National Aeronautics and Space Administration Cleveland, Ohio 44135		10. Work Unit No. 501-24 11. Contract or Grant No.
12. Sponsoring Agency Name and Address National Aeronautics and Space Administration Washington D. C. 20546		13. Type of Report and Period Covered Technical Note 14. Sponsoring Agency Code
15. Supplementary Notes		

16. Abstract

Data were taken with a film-cooled test plate placed in the exhaust stream of a rectangular combustor. Results showed that in a fuel-rich zone, fuel entrained into the film-cooling air would burn at the conditions tested. Test conditions were cooling-gas flow rates, 9.5 and 5 percent of total gas flow; cooling-gas velocities, 23 and 12 m/sec (75 and 40 ft/sec); ambient-temperature cooling gas; hot-gas velocity, nominally 215 m/sec (700 ft/sec); fuel-air ratio to stoichiometric fuel-air ratio values of 0.1, 0.8, 1.0, 1.2, and 1.35, resulting in hot-gas temperatures from 590 to 2100 K (600° to 3300° F); atmospheric pressure. Analytical prediction of wall temperatures agreed reasonably well with experimental results.

17. Key Words (Suggested by Author(s))	18. Distribution Statement		
Film cooling Combustor Heat transfer Fuel-rich	Unclassified - unlimited		
19. Security Classif. (of this report) Unclassified	20. Security Classif. (of this page) Unclassified	21. No. of Pages ~~34~~ 36	22. Price* Domestic, $3.00 Foreign, $5.50

* For sale by the National Technical Information Service, Springfield, Virginia 22151

FILM COOLING IN A COMBUSTOR OPERATING AT FUEL-RICH EXIT CONDITIONS

by Robert R. Tacina and Cecil J. Marek

Lewis Research Center

SUMMARY

Data were taken to determine whether fuel entrained into a film-cooling layer would burn. Ambient-temperature air was injected tangentially as a film above a test plate through a single film-cooling slot, 0.64 centimeter (0.25 in.) high. The test plate was placed in the exhaust stream of a rectangular combustor. Temperatures of the test plate were used to deduce that, in a fuel-rich zone, entrained fuel would burn with the film-cooling air at the conditions tested. Visual observation of the film also indicated burning. Nitrogen cooling data were taken and used for comparison. Analytical calculations were made and agreed reasonably well with the experimental results. Test conditions were cooling-gas flow rates, 9.5 and 5 percent of total gas flow; cooling-gas velocities, 23 and 12 m/sec (75 and 40 ft/sec); ambient-temperature cooling gas; hot-gas velocity, nominally 215 m/sec (700 ft/sec); fuel-air ratio to stoichiometric fuel-air ratio values of 0.1 0.8, 1.0, 1.2, and 1.35; atmospheric pressure.

INTRODUCTION

This study was conducted to determine whether, in a fuel-rich zone, the fuel entrained into the film-cooling air would burn, and if it did burn, to determine the degradation of the film-cooling effectiveness. No effort was made to establish criteria for when the entrained fuel would or would not burn.

Film cooling is presently the primary method of cooling liner walls in combustors of gas turbine engines. If fuel would be entrained into the cooling air in a fuel-rich zone and then burn, the cooling effectiveness would be much lower. Generally, gas turbines are well below overall stoichiometric fuel-air ratio. However, in the primary zone of the combustor the local fuel-air ratios are nearly stoichiometric, and there may be regions where the film-cooling air is injected into a fuel-rich zone. There is also research being done for advanced engines in which the combustor would be operated at fuel rich

conditions. At the resulting high temperatures the turbine blades will require film cooling (ref. 1). In this case, film cooling in a fuel-rich zone would occur in the combustor and on the turbine blades.

In the experiment reported herein, ambient-temperature air was tangentially injected as a film above a test plate through a single film-cooling slot. The test plate was located in the exhaust stream of a sector combustor operated at atmospheric pressure. Data were taken at hot-gas equivalence ratios (fuel-air ratio to stoichiometric fuel-air ratio) ranging from 0.1 to 1.35, resulting in hot-gas temperatures from 590 to 2100 K (600° to 3300° F). Cooling-gas flows of 5 and 9.5 percent of the hot-gas flows were used. The velocity of the hot-gas stream was approximately 215 m/sec (700 ft/sec), while the velocity of the film was approximately 12 or 23 m/sec (40 or 75 ft/sec). Test-plate temperatures were measured along the axial centerline of the plate. These temperatures were used to deduce whether burning occurred in the cooling film. Visual observation of the test plate was also possible. Data with nitrogen cooling, which precluded burning in the film layer, were taken for comparison.

An analytical model was developed to calculate the test-plate temperatures. The temperature of the film cooling stream was calculated using the turbulent mixing model developed in reference 2. In a fuel-rich zone, it was assumed that the fraction of hot gas and fuel entrained in the film would mix and burn. The temperature of the film (including entrained hot gas) would then be increased by the heat of combustion.

All the tests and calculations performed in this study were done in the U.S. customary system of units. The International System of Units (SI) was added for reporting purposes.

ANALYSIS

An analytical model was developed to calculate the test-plate temperatures. The main purpose of the calculations was to investigate the interaction of the various modes of heat transfer and to indicate trends. Considered in the model were the effects of film cooling, hot-gas radiation, casing radiation, convection, and axial wall conduction. The model was essentially the one presented in reference 3. To calculate the effect of film cooling on the wall temperatures, the turbulent mixing model of reference 2 was used. The details of the calculation procedure are given in appendix A.

In this report the effect of entrained fuel burning in the film-cooling stream was added to the calculation of the film-cooling effectiveness. Entrained fuel was assumed to burn with the film-cooling air whenever the hot-gas fuel air ratio was stoichiometric or greater. Fuel resulting from the inefficiency of the combustor was assumed not to burn in the film stream at fuel-air ratios below stoichiometric. With nitrogen cooling, none of the entrained fuel burned. For details, see the discussion under Film Temperature in appendix A.

APPARATUS AND INSTRUMENTATION

Flow System

Figure 1 is a schematic of the flow system used. The airflow was measured with a square-edged orifice. A vitiated preheater raised the temperature of the air to 590 K (600° F). A plenum, followed by a set of screens, provided a uniform velocity profile at the combustor inlet. For safety pruposes when running fuel-rich, oxygen was introduced downstream of the test section to burn the excess fuel. The hot combustion gas then was water quenched and exhausted to the atmosphere.

The air or notrogen cooling flow for the test section was separately metered. It entered the test section at ambient temperature and atmospheric pressure through a continous film-cooling slot.

Combustor and Test Section

A rectangular combustor operated at atmospheric pressure was used to generate the hot gas. A sketch of the combustor and test section is shown in figure 2. The fuel for the combustor was ASTM-A-1. The fuel was injected upstream of the flameholders by simplex nozzles with a spray angle of 90°. There were three rows of four nozzles. Three V-gutters, which provided 80 percent blockage, were used as flameholders. With this high blockage, good efficiencies at high fuel-air ratios were obtained. A plot of combustion efficiency against overall equivalence ratio is shown in figure 3(a). In figure 3(b) the combustor exhaust temperatures are shown as a function of overall equivalence ratio.

Air or nitrogen cooling flow was introduced downstream of the combustor through a continuous slot. The film-cooling-slot lip was formed into a knife-edge to minimize the slot blockage, which might perform as a flameholder. The height of the cooling slot exit was 0.64 centimeter (0.25 in.). The test plate was 25 by 38 by 0.32 centimeter (10 by 15 by 0.125 in.) type 304 stainless steel. The undersurface of the test plate was insulated with a 1-centimeter (0.4-in.) layer of an alumina-silica compound with a thermal conductivity of 0.14 watt/(m)(K) at 1033 K (0.08 Btu/(hr)(ft)($^{\circ}$F) at 1400°F). An air gap of 2.2 centimeter (0.88 in.) existed between the insulation and the casing wall. A quartz window was provided for viewing the test plate. This window was cooled by a separate ambient-temperature air film. The walls of the combustor and test section were jacketed and cooled with water. The test-section hardware (without water jacket and test plate) is shown in figure 4.

Instrumentation

Static and total pressure measurements were made at the combustor inlet to check the velocity profile. The hot-gas temperature and velocity at the exit of the test section were measured at 40 points with a combined total pressure - total temperature traversing probe. The temperature probe was a cooled-gas inferential probe that is described in appendix B. Test-plate temperatures were measured along the axial centerline every 2.54 centimeters (1.0 in.) by Chromel-Alumel thermocouples. The first thermocouple was directly beneath the knife-edge. These thermocouples were placed on the undersurface of the test plate before the insulation was installed.

RESULTS AND DISCUSSION

Tests were made to determine whether fuel entrained into the film-cooling air layer would burn. The procedure to determine whether there was burning consisted of recording the temperatures along a film-cooled test plate. If the temperature of the test plate kept rising as the hot-gas fuel-air ratio went above stoichiometric, it was assumed the entrained fuel was burning. Film cooling with nitrogen was then run at the same flow rates and fuel-air ratios. Since the nitrogen film could not support combustion, the nitrogen cooling data could be used to confirm the results with air cooling.

The test conditions are presented in table I. Excessive wall temperatures prohibited data being taken at cooling flows lower than 5 percent . The hot-gas equivalence ratio of 0.1 in table I corresponds to the preheat condition. Combustor and film-cooling data are given in table II. Note that not all the data are presented in the figures. To make the figures readable, only the preheat condition, the stoichiometric condition, and the 1.3-equivalence-ratio condition are plotted. The data for the intermediate conditions are in table II.

The results for the 9.5 and 5 percent cooling-gas flows are discussed separately, followed by a discussion of the effect on film temperature of entrained fuel burning with the film-cooling air (based on analytical results).

Data for 9.5 Percent Cooling-Gas Flow

Figure 5 shows the test-plate temperatures as a function of axial distance from the knife-edge for the 9.5 percent cooling-gas flow and three equivalence ratios. In figure 5(a) the test-plate temperature continued to increase as the hot-gas equivalence ratio went above stoichiometric, indicating that burning occurred in the cooling airstream.

Definitions of symbols appearing in figure 5 and in further discussion are presented in appendix C.

Visual observations also indicated that burning occurred in the cooling airstream. At high temperatures the hot-gas stream gave a blue flame appearance, indicating nonluminous combustion and the absence of smoke. As the fuel-air ratio went above stoichiometric, the flame attained a whitish radiance, which existed in addition to the blue flame background. Also at above stoichiometric fuel-air ratios a blue flame front developed above the test plate, originating at the knife-edge. As the fuel-air ratio increased, the flame front became brighter and larger. This flame front indicated that there was burning in the cooling airstream.

The agreement was fair between the experimental values and the calculated results. A turbulent mixing coefficient C_m (see eq. (A16) in appendix A) of 0.05 best fit the data. This value was held constant for the rest of the calculations. The value of C_m seems to be independent of the hot-gas temperature. At the fuel-rich condition, the calculated results near the slot were well below the experimental values. Downstream of the 7.6-centimeter (3-in.) location, the calculated results were well above the experimental values. Since the purpose of the calculations was to show trends, no further effort was made to improve the agreement between the calculated and experimental results.

Experimental check data were taken on another day with air cooling, and burning in the film air at the fuel-rich conditions did not occur. The results are presented in figure 5(b). The test was again repeated at a later date, and the results were similar to those of figure 5(a), again indicating burning in the film. One explanation is that this was a condition where the burning was unstable, and a slight change in conditions might cause the film to burn (or not to burn). One slight change was that the inlet cooling air temperature was about 22 K (40° F) lower when the film did not burn.

Comparison of the nitrogen cooling data, figure 5 (c), with the air cooling data, figure 5(a), again indicates that burning in the cooling airstream did occur at the fuel-rich conditions. At a hot-gas equivalence ratio of 1.3 the test-plate temperatures with air cooling are 225 K (400° F) higher than the test-plate temperatures with nitrogen cooling. The change in test-plate temperatures at a hot-gas equivalence ratio of 1.3 is clearly shown in figure 6, which is a cross-plot of the test-plate temperatures at 12.7 centimeters (5.0 in.) from the knife-edge against hot-gas equivalence ratio.

Data for 5 Percent cooling-Gas Flow Rate

Test-plate temperature data with 5 percent air cooling and nitrogen cooling are shown in figure 7. Again the temperature data indicated that the fuel entrained in the cooling air burned at overstoichiometric conditions. Visual results also indicated burning in the cooling airstream.

The effect of entrained fuel burning on the test-plate temperature is shown in figure 8, which is a crossplot of the test-plate temperatures at the 12.7-centimeter (5-in.) location against the hot-gas equivalence ratio. Good agreement exists between the air cooling and nitrogen cooling results to a stoichiometric fuel-air ratio ($\varphi^* = 1$). Above stoichiometric fuel-air ratios ($\varphi^* > 1$), entrained fuel burns in the film-cooling airstream and the plate termperature continues to rise with hot-gas equivalence ratio. The test-plate temperatures with air cooling are 167 K (300° F) higher than the test-plate temperatures with nitrogen cooling at an equivalence ratio of 1.3.

The analytical results show the same trends as the experimental data and agree within ±20 percent, as shown in figure 7. The difference between the analytical and experimental results is attributed to test-plate and knife-edge warpage. This warpage became visibly evident as cooling flows lower than 5 percent were tried.

Effect of Film Burning on Film Temperature

To illustrate the extent that the film temperature can be raised with burning, the calculated film temperatures are plotted in figure 9, along with the calculated test-plate temperatures. At a distance from the knife-edge of 12.7 centimeters (5 in.) or greater, burning was calculated to increase the film temperature by more than 400 K (720°F) as the hot-gas equivalence ratio went from 1.0 to 1.3. The test-plate temperatures, however, show only a 200 K (360° F) temperature rise as the hot-gas equivalence ratio went from 1.0 to 1.3. The reason for this was that as the test-plate temperature increased, radiation to the opposite wall (it was water jacketed) increased, thus reducing the effect of the increased film temperature.

At the 5 percent air cooling flow rate (fig. 9(b)) the calculated film temperature became greater than the measured hot-gas temperature at the fuel-rich condition. The calculated film temperature approached the stoichiometric temperature of 2290 K (3600° F). The presence of fuel in the cooling-gas stream can significantly increase the film temperature.

CONCLUDING REMARKS

Combustor operating conditions usually comprise lower hot-gas velocities, higher inlet film-cooling temperatures, and higher pressures than those used in this study. Such conditions would be more favorable for burning in the film than the conditions used in this study. The entrainment rate of fuel and hot gas into the film-cooling stream may be different from those encountered herein. The entrainment rate is given by: $\dot{m}'_e = C_m \rho_H u_H$. In a combustor, the turbulent mixing coefficient C_m may be about the same, hot-gas density ρ_H would probably be higher with higher pressure, and hot-gas velocity u_H would probably be lower. The net effect may be an entrainment rate approximately equal to the rate in this study. Thus, any fuel entrained into the cooling film could be expected to burn in a combustor.

SUMMARY OF RESULTS

Data were taken with film cooling in a fuel-rich zone. Test conditions were cooling-gas flow rates, 9.5 and 5 percent of total gas flow; cooling-gas velocities, 23 and 12 m/sec (75 and 40 ft/sec); ambient-temperature cooling gas; hot-gas velocity, 215 m/sec (700 ft/sec); hot-gas equivalence ratios, 0.1, 0.8, 1.0, 1.2, and 1.35; atmospheric pressure. The following results were obtained:

1. Fuel entrained into the cooling air burned at the fuel-rich conditions tested.
2. An analytical model assuming instantaneous mixing and complete burning of the entrained fuel with the film air was in reasonable agreement with experimental results.
3. The turbulent mixing coefficient was independent of hot-gas temperature.

Lewis Research Center,
National Aeronautics and Space Administration,
Cleveland, Ohio, August 29, 1973,
501-24.

APPENDIX A

HEAT-TRANSFER MODEL

The development of the heat-transfer model follows closely that in reference 3. The differences in this model are in the correlation used to calculate the film temperatures and in the equations used for wall conduction at the boundary conditions. The heat-flux components at any point x are shown in figure 10. The basic equation is a steady-state energy balance on the plate. The radiation flux and convection from the flame to the plate at point x are equated with the radiation from the plate to the casing and the net conduction at point x. These equations are given in this appendix.

Energy Balance

The energy balance equation is

$$R_i + C_i + KC_i = R_o + C_o + KC_o \tag{A1}$$

Let the net wall conduction be

$$KC = KC_i - KC_o \tag{A2}$$

then

$$R_i - R_o + C_i - C_o + KC = 0 \tag{A3}$$

Radiation from Flame to Test Plate

The radiation from a flame at temperature T_H to a black wall at temperature T_W is given by

$$R_i = \sigma\left(\epsilon_H T_H^4 - \alpha_H T_w^4\right) \tag{A4}$$

Since the wall is not black, reference 3 uses a correction term suggested by McAdams, $\frac{1}{2}(1 + \alpha_w)$, as well as an empirical formula by Lefebvre and Herbert

$$\frac{\alpha_H}{\epsilon_H} = \left(\frac{T_H}{T_w}\right)^{1.5} \tag{A5}$$

Then equation (A4) can be written as

$$R_i = \sigma \left(\frac{1 + \alpha_w}{2}\right) \epsilon_H T_H^{1.5} \left(T_H^{2.5} - T_w^{2.5}\right) \tag{A6}$$

Let

$$A = \sigma \left(\frac{1 + \alpha_w}{2}\right) \epsilon_H T_H^{1.5} \tag{A7}$$

Then

$$R_i = A \left(T_H^{2.5} - T_w^{2.5}\right) \tag{A8}$$

The wall absorptivity α_w was set equal to 0.85 for stainless steel.

Emissivity of Flame

Reeves' correlation for a nonluminous distillate fuel as given in reference 3 was used,

$$\epsilon_H = 1 - \exp\left[-18.5\, p \left(L_B \frac{f}{a}\right)^{0.5} T_H^{-1.5}\right] \tag{A9}$$

where the units are p - lbf/ft^2, L_B - feet, and T_H - degrees Rankine.

Radiation from Test Plate to Casing

Assuming the test-plate and upper casing surface areas are equal,

$$R_o = \sigma \left[\frac{\epsilon_w \epsilon_c}{\epsilon_c + \epsilon_w(1 - \epsilon_c)}\right] \left(T_w^4 - T_c^4\right) \tag{A10}$$

Let

$$B = \sigma \left[\frac{\epsilon_w \epsilon_c}{\epsilon_c + \epsilon_w(1 - \epsilon_c)}\right] \tag{A11}$$

then

$$R_o = B\left(T_w^4 - T_c^4\right) \tag{A12}$$

The wall emissivity e_w was taken to be 0.85, and the casing emissivity ϵ_c was taken to be 0.8.

Conduction Along Test Plate

The axial heat flux along the test plate can be approximated numerically by

$$KC = \delta_w k_w \frac{d^2T}{dx^2} \cong \delta_w k_w \left(\frac{T_{w_{I+1}} + T_{w_{I-1}} - 2T_{w_I}}{(\Delta x)^2}\right) \tag{A13}$$

where the subscript on T_w refers to the increment along the test plate. The wall thickness δ_w was 0.318 centimeter (0.125 in.), and the thermal conductivity k_w was taken to be 24 watt/(m)-(K) (14 Btu/(ft)-(hr)-(^oF)).

Convection to Test Plate

The convective heat flux to the test plate can be written as

$$C_i = h\,(T_f - T_w) \tag{A14}$$

where

$$h = \frac{k}{\bar{x}}\,(0.0365)\,Re_x^{0.8}Pr^{0.4} \tag{A15}$$

In equations (A15), Re_x and Pr were calculated at the film conditions.

Film Temperature

The film temperature can be calculated if the amount of entrained hot gas is known. A sketch of the one-dimensional model used is presented in figure 11. It was assumed that the hot gas is entrained into the film-cooling airstream and mixes with it. When the hot gas entrained into the film-cooling airstream is fuel rich, it is also assumed that all the entrained fuel burns instantaneously. The entrainment rate per unit area is assumed to be related to the hot-gas mass flux by the turbulent mixing coefficient C_m (ref. 2),

$$\dot{m}'_e = C_m \rho_H u_H \tag{A16}$$

Let $\dot{m}_e$ be the total mass entrained at any axial position x, then

$$\dot{m}_e = \int_0^{Wx} \dot{m}'_e \, dA = \dot{m}'_e Wx = C_m \dot{m}_H \frac{x}{y} \tag{A17}$$

The mass flow of the film stream would then be $\dot{m}_s + \dot{m}_e$, and the fuel-air ratio of the film would be

$$\left(\frac{f}{a}\right)_{film} = \left(\frac{f}{a}\right)_H \frac{\dot{m}_e}{\dot{m}_s + \dot{m}_e} \tag{A18}$$

Then the film temperature was calculated from the inlet temperature and the fuel-air ratio of the film. (The inlet temperature to the preheater and the slot temperature of the cooling air were approximately the same.) This procedure to calculate the film temperature was used to avoid the problem of varying specific heats.

Fuel resulting from the inefficiency of the combustor was assumed not to burn in the film stream for hot-gas conditions below stoichiometric and for the nitrogen cooling tests. To correct the film fuel-air ratio for this unburned fuel, an equivalent hot-gas fuel-air ratio was used such that the theoretical temperature of the hot-gas would equal the actual temperature of the hot gas. In the fuel-rich case with air cooling, all the entrained fuel was assumed to burn and thus the actual fuel-air ratio was used.

Heat Loss Through Insulation

The heat flux through the insulation is approximated by

$$C_o \cong \frac{k_{ins}}{\delta_{ins}} (T_w - T_{ins}) \tag{A19}$$

The value of T_{ins} was found by equating C_o with the heat transfer through the air gap between the insulation and the casing (fig. 10). Since it was assumed that there was not any circulation in the air gap, the heat transfer there was considered to be by conduction.

$$C_o = \frac{k_{ins}}{\delta_{ins}}(T_w - T_{ins}) = \frac{k_{air}}{\delta_{air}}(T_{ins} - T_c) = \frac{T_w - T_c}{\frac{\delta_{ins}}{k_{ins}} + \frac{\delta_{air}}{k_{air}}} \quad \text{(A20)}$$

The value for the temperature of the lower casing wall T_c was assumed to be 373 K (212^o F).

Method of Solution

The preceding equations can be substituted into the overall energy equation (A3), giving

$$A\left(T_H^{2.5} - T_{w_I}^{2.5}\right) - B\left(T_{w_I}^4 - T_c^4\right) + h\left(T_f - T_{w_I}\right) + k_w\delta_w\left[\frac{T_{w_{I+1}} + T_{w_{I-1}} - 2T_{w_I}}{(\Delta x)^2}\right] - \frac{T_{w_I} - T_c}{\frac{\delta_{ins}}{k_{ins}} + \frac{\delta_{air}}{k_{air}}} = 0 \quad \text{(A21)}$$

or

$$D_1 T_{w_I}^4 + D_2 T_{w_I}^{2.5} + D_3 T_{w_I} = D_4 \quad \text{(A22)}$$

where D_1, D_2, D_3, and D_4 are known and

$$D_1 = B \quad \text{(A23)}$$

$$D_2 = A \quad \text{(A24)}$$

$$D_3 = h + \frac{2k_w\delta_w}{(\Delta x)^2} + \frac{1}{\frac{\delta_{ins}}{k_{ins}} + \frac{\delta_{air}}{k_{air}}} \quad \text{(A25)}$$

$$D_4 = AT_H^{2.5} + BT_c^4 + hT_f + \frac{k_w \delta_w}{(\Delta x)^2}\left(T_{w_{I+1}} + T_{w_{I-1}}\right) + \frac{T_c}{\frac{k_{ins}}{\delta_{ins}} + \frac{k_{air}}{\delta_{air}}} \tag{A26}$$

Equation (A22) can be solved numerically at each point by using Newton's method.

Boundary Conditions

The test plate extends upstream under the knife-edge and was assumed to behave as a fin with an effective length $N_{fin}\delta_w$ (see fig. 12(a)). The heat conducted into the fin must be transferred to the film-cooling stream by convection. Then the energy balance at $x = 0$ is

$$\begin{pmatrix}\text{Radiation from}\\ \text{flame to test}\\ \text{plate}\end{pmatrix} - \begin{pmatrix}\text{Radiation from}\\ \text{test plate}\\ \text{to casing}\end{pmatrix} + \begin{pmatrix}\text{Net conduction}\\ \text{into cell}\end{pmatrix} - \begin{pmatrix}\text{Heat transfer}\\ \text{through insulation}\\ \text{to casing}\end{pmatrix} = \begin{pmatrix}\text{Convection from fin and}\\ \text{cell at } x = 0\end{pmatrix}$$

or

$$A\left(T_H^{2.5} - T_{w_1}^{2.5}\right) - B\left(T_{w_1}^4 - T_c^4\right) + \frac{k_w \delta_w W\left(T_{w_2} - T_{w_1}\right)}{(\Delta x)^2 W} - \frac{T_{w_1} - T_c}{\frac{\delta_{ins}}{k_{ins}} + \frac{\delta_{air}}{k_{air}}} = \frac{h}{(\Delta x)W}\left[N_{fin}\delta_w W + \frac{1}{2}(\Delta x)W\right]\left(T_{w_1} - T_s\right) \tag{A27}$$

A value of 1 for N_{fin} best fit the data.

The end of the test plate was assumed to be insulated as in figure 12(b). There the energy balance at $x = \ell$ is

$$\begin{pmatrix}\text{Radiation from flame}\\ \text{to test plate}\end{pmatrix} - \begin{pmatrix}\text{Radiation from test}\\ \text{plate to casing}\end{pmatrix} + \begin{pmatrix}\text{Convection from}\\ \text{film to test plate}\end{pmatrix} + \begin{pmatrix}\text{Conduction}\\ \text{into cell}\end{pmatrix} - \begin{pmatrix}\text{Heat transfer through}\\ \text{insulation to casing}\end{pmatrix} = 0$$

or

$$A\left(T_H^{2.5} - T_{w_N}^{2.5}\right) - B\left(T_{w_N}^4 - T_c^4\right) + h\left(T_{f_N} - T_{w_N}\right) + 2\,\frac{k_w \delta_w}{(\Delta x)^2}\left(T_{w_{N-1}} - T_{w_N}\right)$$

$$- \frac{T_{w_N} - T_c}{\frac{\delta_{ins}}{k_{ins}} + \frac{\delta_{air}}{k_{air}}} = 0 \qquad \text{(A28)}$$

APPENDIX B

INFERENTIAL TEMPERATURE PROBE

A cooled-gas pyrometer was used to measure the hot-gas temperatures. The standard bare-wire thermocouples were not suitable because of the high temperature, 2250 K (3600° F), and the oxidizing atmosphere in the combustor exhaust. The principle of the cooled-gas pyrometer is to cool the hot-gas and then measure the gas temperature with a thermocouple. The gas is cooled by flowing through a tube with water-cooled walls. Figure 13 is a sketch of the probe.

To calculate the free-stream temperature from the measured temperature, the temperature drop of the gas has to be calculated. The amount of this temperature drop is a function of flow through the tube, gas properties, tube geometry, and cooling-water temperatures. In reference 4 the theory for a cooled-gas pyrometer was developed. The "working" equation for the probe was shown to be

$$\ln\left(\frac{T_0 - T_{wa}}{T_2 - T_{wa}}\right) = \left(K\,Pr^{-2/3}\right) f(M, \gamma)^{-a_1} \left[\frac{P_0}{\frac{\mu_2}{\mu_r}\sqrt{\frac{T_2}{T_r}}}\right]^{-a_1}$$

where

$$f(M, \gamma) = \sqrt{M\gamma}\left(\frac{2}{\gamma+1}\right)^{\frac{\gamma+1}{2\gamma-1}}$$

The subscripts 0 and 2 refer to station numbers shown in figure 13.

To calibrate the probe, if T_0, T_{wa}, T_2, and P_0 are known at a number of calibration points, then $\log\left\{\ln\left[(T_0 - T_{wa})/(T_2 - T_{wa})\right]\right\}$ can be plotted against $\log\left\{f(M, \gamma)\left[P_0/(\mu_2/\mu_r)\sqrt{T_2/T_r}\right]\right\}$. The value of a_1 can be found from the slope and the value of $(K\,Pr^{-2/3})$ from the intercept. A calibration curve for the probe used in this report is shown in figure 14. The data used for the curve are listed in table III.

APPENDIX C

SYMBOLS

A	defined by eq. (A7)
B	defined by eq. (A11)
C	convective heat flux
C_m	turbulent mixing coefficient
D_1	defined by eq. (A23)
D_2	defined by eq. (A24)
D_3	defined by eq. (A25)
D_4	defined by eq. (A26)
f/a	fuel-air ratio
h	convective heat-transfer coefficient
K	constant
KC	thermal conductive heat flux
k	thermal conductivity
l	length of test plate
L_B	mean beam path length
M	molecular weight
$\dot{m}_e$	total entrained mass flow rate at point x
$\dot{m}'_e$	mass entrained per unit area per unit time
$\dot{m}_s$	mass flow rate through slot
N_{fin}	fin factor
P	static pressure
P_0	total pressure at station 0 of cooled-gas pyrometer
Pr	Prandtl number
R	radiation heat flux

Re	Reynolds number
S	slot height
T	temperature
T_{w_I}	wall temperature at increment I
u	velocity
W	width of combustor
x	axial distance from knife-edge
Δx	incremental length along test-plate axial centerline
y	height of combustor
α_H	absorptivity of hot gas at T_H
α_w	absorptivity of wall at T_w
γ	specific-heat ratio
δ	thickness
ϵ	emissivity
η_c	combustion efficiency in percent, $\frac{\text{Actual temperature rise}}{\text{Theoretical temperature rise}} \times 100$
μ	viscosity
ρ	mass density
σ	Stefan-Boltzmann constant
φ	overall equivalence ratio, $\frac{\text{Fuel flow}}{(\text{Combustion airflow})+(\text{Cooling flow})} \Big/ 0.068$
φ^*	hot-gas equivalence ratio, $\frac{\text{Fuel flow}}{\text{Combustion airflow}} \Big/ 0.068$

Subscripts:

air	properties of air in air gap between casing and insulation
c	casing
e	entrained
f	film
H	hot gas
i	in

ins	insulation
N	last wall increment
o	out
r	reference
s	film at slot exit
st	stoichiometric
w	wall (test plate)
wa	water
x	at distance x
0	station 0 of cooled-gas pyrometer
2	station 2 of cooled-gas pyrometer

REFERENCES

1. Esgar, Jack B.; Colladay, Raymond S.; and Kaufman Albert: An Analysis of the Capabilities and Limitations of Turbine Air Cooling Methods. NASA TN D-5992, 1970.

2. Juhasz, Albert J.; and Marek, Cecil J.: Combustor Liner Film Cooling in the Presence of High Free-Stream Turbulence. NASA TN D-6360, 1971.

3. Anon.: Computer Program for the Analysis of Annular Combustors. Vol. 1: Calculation Procedures. Rep. 1111-1, vol. 1, Northern Research and Engineering Corp. (NASA CR-72374), Jan. 29, 1968.

4. Krause, Lloyd N.; Johnson, Robert C.; and Glawe, George E.: A Cooled-Gas Pyrometer for use in High-Temperature Gas Streams. NACA TN 4383, 1958.

TABLE I. - TEST CONDITIONS

Hot-gas flow, kg/sec (lbm/sec)	1.36 (3)
Hot-gas velocity through test section, m/sec (ft/sec)	215 (700)
Cooling-gas flow rate, kg/sec (lbm/sec)	0.136, 0.0725 (0.3, 0.16)
Hot-gas equivalence ratios	0.1, 0.8, 1.0, 1.2, 1.35
Pressure, atm	1

TABLE II. - COMBUSTOR AND FILM COOLING DATA

(a) SI units

Combustor flow rate, kg/sec	Equivalence ratio		Hot-gas temperature, K	Combustion efficiency	Cooling gas	Cooling-gas flow rate, kg/sec	Cooling-gas temperature, K	Ratio of cooling gas flow to total flow, percent	Axial distance from knife-edge, cm										
	Overall	Hot-gas							0	2.54	5.08	7.62	10.16	12.70	15.24	17.78	20.82	22.86
									Test-plate temperature, K									
1.35	0.106	0.116	539	----	Air	0.133	297	8.98	309	333	365	388	402	410	---	---	422	411
1.38	.735	.809	1812	91.4		.144	294	9.44	473	542	637	748	818	856	---	---	943	900
1.37	.894	.988	2070	93.8		.145	295	9.54	511	584	679	794	868	910	---	---	1025	974
1.38	1.042	1.154	2001	84.3		.145	296	9.54	529	589	667	773	854	906	---	---	1043	976
1.38	1.190	1.315	1841	78.1		.146	296	9.55	610	657	977	1032	1077	1113	---	---	1210	1172
1.37	.101	.111	562	----		.144	276	9.53	307	329	359	385	404	419	---	432	434	419
1.38	.744	.818	1878	95.5		.144	276	9.42	481	536	589	649	712	772	---	897	926	867
1.35	.905	1.000	2086	94.2		.145	277	9.17	514	572	623	682	749	815	---	949	982	921
1.36	1.061	1.177	2077	88.8		.147	277	9.75	519	573	631	704	781	855	---	986	1031	995
1.35	1.230	1.315	1874	80.0		.145	277	9.72	497	544	597	668	757	842	---	994	1032	989
1.39	.093	.101	577	----	N_2	.139	253	9.09	284	302	330	354	372	384	394	404	406	392
1.34	.760	.842	1929	97.0		.137	266	9.30	466	526	587	649	718	782	844	904	933	874
1.38	.905	.996	2057	92.5		.134	266	8.90	501	566	628	697	782	854	924	989	1023	954
1.36	1.069	1.179	1967	82.4		.139	269	9.25	509	569	631	707	797	871	941	1002	1033	968
1.36	1.245	1.375	1847	78.2		.133	270	8.90	484	544	620	706	791	854	914	967	994	946
1.38	.106	.111	554	----	Air	.0722	282	4.96	319	342	378	406	424	437	---	452	453	443
1.36	.778	.820	1884	92.0		.0735	282	5.12	600	688	865	1003	1083	1123	---	1176	1188	1157
1.36	.958	1.007	2068	89.9		.0735	283	5.11	657	751	951	1002	1181	1217	---	1271	1284	1248
1.34	1.124	1.185	2000	85.6		.0740	284	5.21	663	784	1004	1152	1229	1264	---	1315	1326	1262
1.38	1.268	1.333	1886	83.3		.0731	284	5.05	703	854	1060	1192	1259	1289	---	---	1342	1263
1.35	.107	.113	546	----	N_2	.0658	292	4.66	316	348	---	418	434	446	---	---	464	454
1.38	.781	.823	1851	88.9		.0720	294	4.91	668	781	---	1073	1122	1147	---	---	1204	1187
1.34	.993	1.044	2084	89.4		.0658	294	4.69	787	935	---	1218	1264	1287	---	---	1304	1179
1.38	1.101	1.158	1944	81.4		.0633	294	4.60	762	847	---	1101	1160	1196	---	---	1262	1237
1.36	1.280	1.348	1819	83.0		.0663	294	4.65	761	833	---	1054	1111	1147	---	---	1207	1191

TABLE II. - Concluded. COMBUSTOR AND FILM-COOLING DATA

(b) U.S. customary units

Combustor flow rate, lbm/sec	Equivalence ratio		Hot-gas temperature, °F	Combustion efficiency	Cooling gas	Cooling-gas flow rate, lbm/sec	Cooling-gas temperature, °F	Ratio of cooling gas flow to total flow, percent	Axial distance from knife-edge, in.									
	Overall	Hot-gas							0	1	2	3	4	5	6	7	8	9
									Test-plate temperature, °F									
2.97	0.106	0.116	511	----	Air	0.293	75	8.98	96	139	197	238	264	278	----	----	299	279
3.05	.735	.809	2801	91.4		.318	69	9.44	391	515	686	886	1013	1081	----	----	1238	1160
3.02	.894	.988	3266	93.8		.319	71	9.54	460	592	763	969	1103	1178	----	----	1385	1294
3.03	1.042	1.154	3141	84.3		.320	72	9.54	492	600	741	932	1078	1170	----	----	1417	1296
3.04	1.190	1.315	2854	78.1		.321	72	9.55	638	1083	1299	1398	1479	1544	----	----	1718	1649
3.01	.101	.111	551	----		.317	37	9.53	93	133	187	233	263	294	----	318	321	294
3.05	.744	.818	2920	95.5		.317	37	9.42	406	504	600	708	821	930	----	1155	1206	1101
2.97	.905	1.000	3295	94.2		.320	38	9.17	465	569	662	767	889	1007	----	1248	1307	1198
2.99	1.061	1.177	3278	88.8		.323	38	9.75	474	572	676	807	946	1079	----	1315	1396	1331
2.97	1.230	1.315	2914	80.0		.320	38	9.72	434	520	614	743	902	1055	----	1329	1397	1290
3.06	.093	.101	578	----	N_2	.305	-5	9.09	51	83	134	177	210	232	249	267	270	245
2.95	.760	.842	3013	97.0		.302	18	9.30	378	487	597	708	833	947	1060	1167	1220	1113
3.04	.905	.996	3243	92.5		.296	18	8.90	442	558	670	795	948	1077	1204	1320	1382	1257
3.00	1.069	1.179	3081	82.4		.306	24	9.25	457	565	676	812	974	1108	1233	1343	1400	1283
3.00	1.245	1.375	2864	78.2		.293	26	8.90	412	519	656	810	963	1078	1185	1280	1330	1243
3.04	.106	.111	538	----	Air	.159	47	4.96	114	156	220	271	304	326	----	353	356	337
3.00	.778	.820	2932	92.0		.162	47	5.12	620	779	1097	1346	1489	1561	----	1656	1679	1623
3.00	.958	1.007	3262	89.9		.162	49	5.11	722	892	1252	1523	1665	1730	----	1827	1852	1787
2.96	1.124	1.185	3140	85.6		.163	51	5.21	733	952	1348	1614	1753	1815	----	1907	1927	1811
3.03	1.268	1.333	2935	83.3		.161	51	5.05	805	1077	1448	1686	1807	1860	----	----	1956	1813
2.97	.107	.113	522	----	N_2	.145	66	4.66	108	166	----	293	321	342	----	----	376	357
3.03	.781	.823	2872	88.9		.155	69	4.91	742	946	----	1471	1560	1604	----	----	1708	1676
2.95	.993	1.044	3292	89.4		.145	69	4.69	957	1223	----	1733	1816	1857	----	----	1887	1663
3.04	1.101	1.158	3040	81.4		.147	69	4.60	911	1065	----	1521	1628	1693	----	----	1812	1767
3.00	1.280	1.348	2815	83.0		.146	69	4.65	910	1039	----	1437	1539	1604	----	----	1713	1683

TABLE III. - COOLED-GAS-PYROMETER CALIBRATION DATA

Temperature at station 0 of cooled-gas pyrometer, T_0		Temperature at station 2 of cooled-gas pyrometer, T_2		Water temperature, T_{wa}		Pressure at station 0 of cooled-gas pyrometer, atm	Fuel-air ratio, f/a	$\log\left[\frac{f(M,\gamma)(P_0 \times 14.7)}{(\mu_2/\mu_r)\sqrt{T_2/556\ K}}\right]$	$\log\left[\ln\left(\frac{T_0 - T_w}{T_2 - T_{wa}}\right)\right]$
K	^oF	K	^oF	K	^oF				
961	1270	432	317	279	42	0.709	0.0241	1.7294	0.1750
1033	1400	442	336	279	42	.721	.0280	1.7257	.1847
1244	1780	481	406	279	43	.721	.0341	1.6809	.1947
1467	2400	516	469	280	44	.709	.0405	1.6363	.2081
1589	2400	532	497	281	45	.980	.0486	1.6236	.2176
1594	2410	567	561	282	47	.980	.0512	1.7313	.1834
1478	2200	546	522	281	46	.988	.0455	1.7513	.1789
1239	1770	499	439	281	45	.988	.0340	1.7960	.1693
1044	1420	461	369	279	43	.980	.0263	1.8359	.1586
800	980	412	281	279	42	.988	.0176	1.8974	.1359
856	1080	413	283	279	42	.988	.0176	1.8959	.1644
794	970	419	295	279	42	1.268	.0180	1.9956	.1138
1022	1380	472	389	280	44	1.268	.0278	1.9343	.1316
1033	1400	477	399	280	44	1.268	.0278	1.9278	.1272
1244	1780	525	485	281	46	1.280	.0398	1.3843	.1379
1489	2220	575	575	283	49	1.287	.0490	1.8413	.1516
1583	2390	594	609	283	50	1.280	.0547	1.8234	.1559
800	980	411	279	278	41	1.110	.0191	1.9502	.1375
800	980	413	283	278	41	1.110	.0191	1.9472	.1322
1022	1380	461	369	279	43	1.113	.0267	1.8925	.1496
1022	1380	467	380	279	43	1.118	.0267	1.8852	.1393
1256	1800	509	456	181	46	1.118	.0375	1.8406	.1624
1478	2200	556	540	282	48	1.118	.0473	1.7976	.1690
1589	2400	575	575	282	48	1.118	.0546	1.7816	.1749
811	1000	401	261	278	40	.845	.0186	1.8445	.1670
1033	1400	444	340	279	42	.838	.0260	1.7869	.1809
1250	1790	487	411	280	44	.851	.0340	1.7454	.1885
1478	2200	526	486	282	47	.815	.0405	1.7067	.2014
1594	2410	544	519	282	47	.845	.0461	1.6870	.2070
1228	1750	502	443	281	46	1.118	.0375	1.8481	.1634

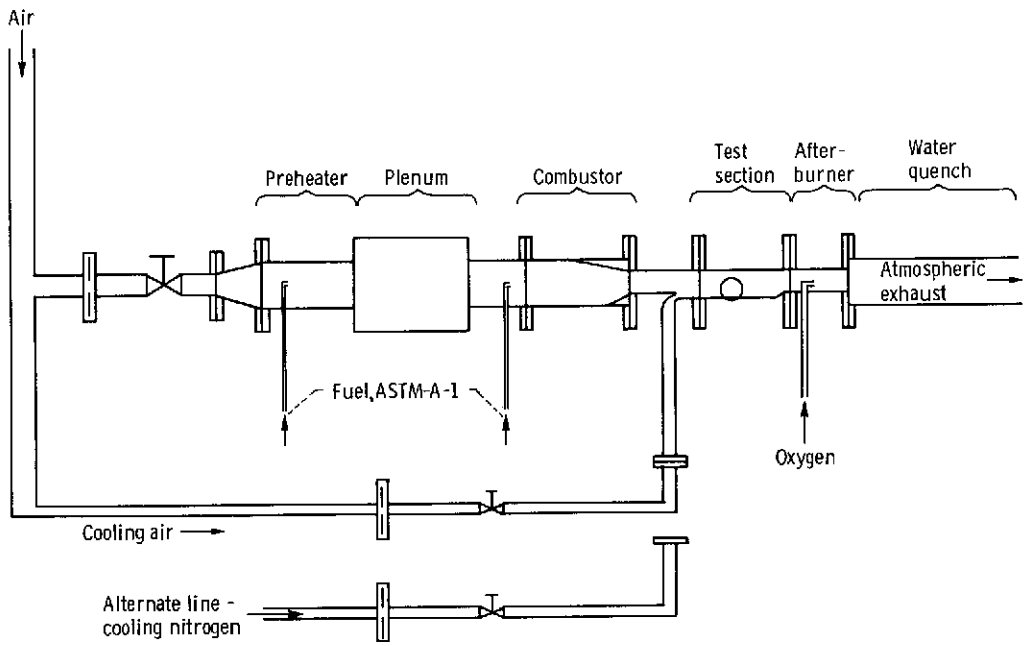

Figure 1. - Schematic of flow system.

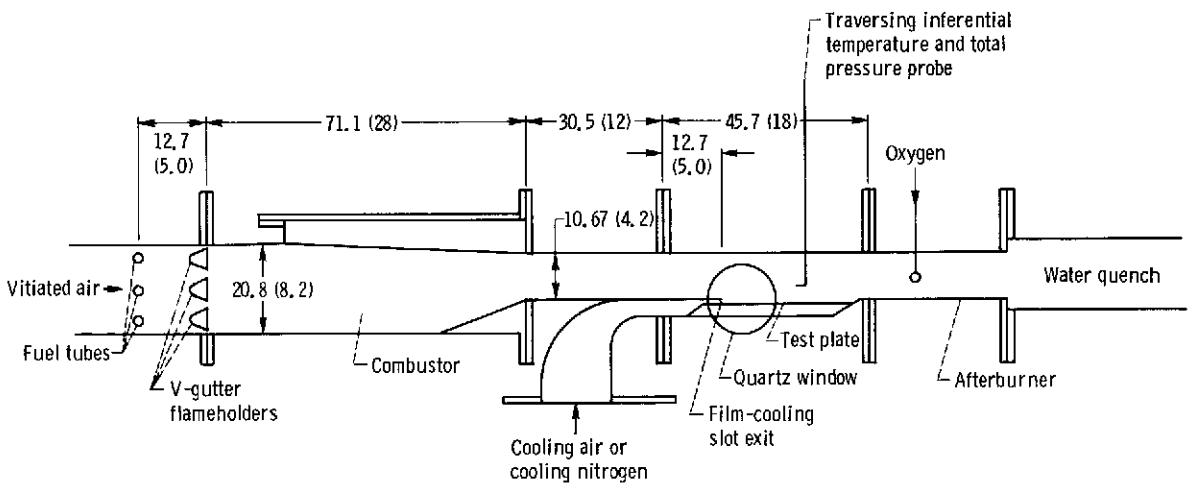

Figure 2. - Schematic of combustor and test section. Dimensions are in centimeters (in.). Width of sections, 38.1 centimeters (15.0 in.).

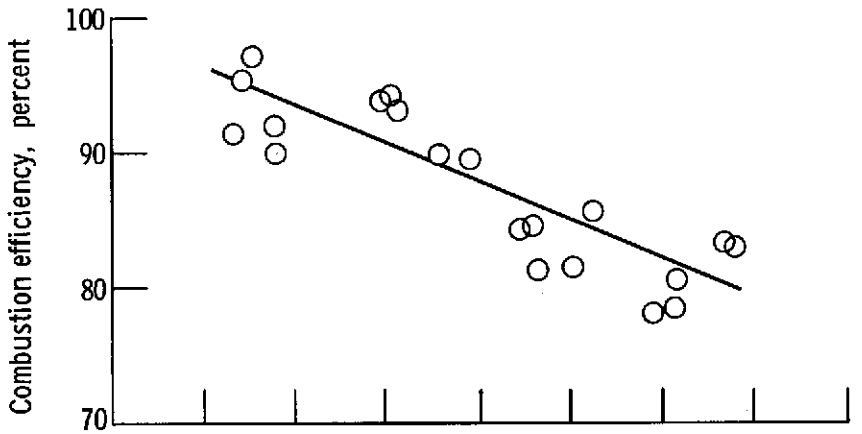

(a) Combustion efficiency at various overall equivalence ratios.

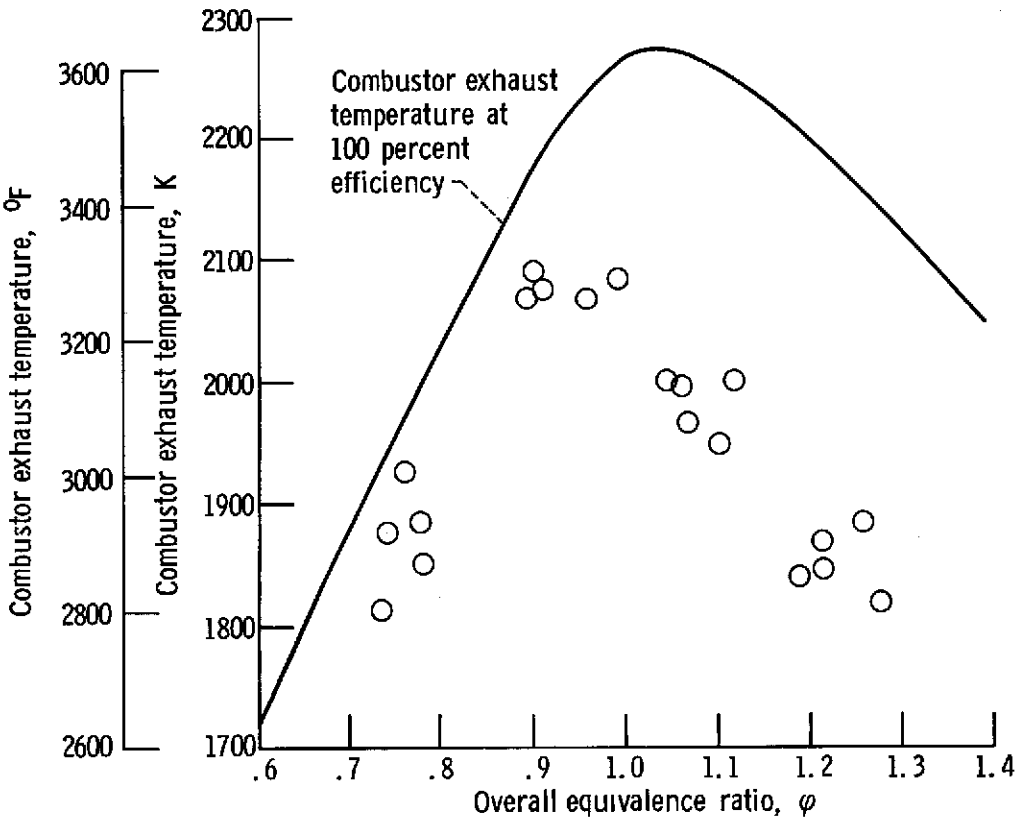

(b) Combustor exhaust temperature at various overall equivalence ratios.

Figure 3. - Combustor performance. Inlet pressure, 1 atmosphere; combustor reference velocity, 23 m/sec (75 ft/sec); inlet temperature from preheater, 590 K (600° F); ambient temperature to preheater.

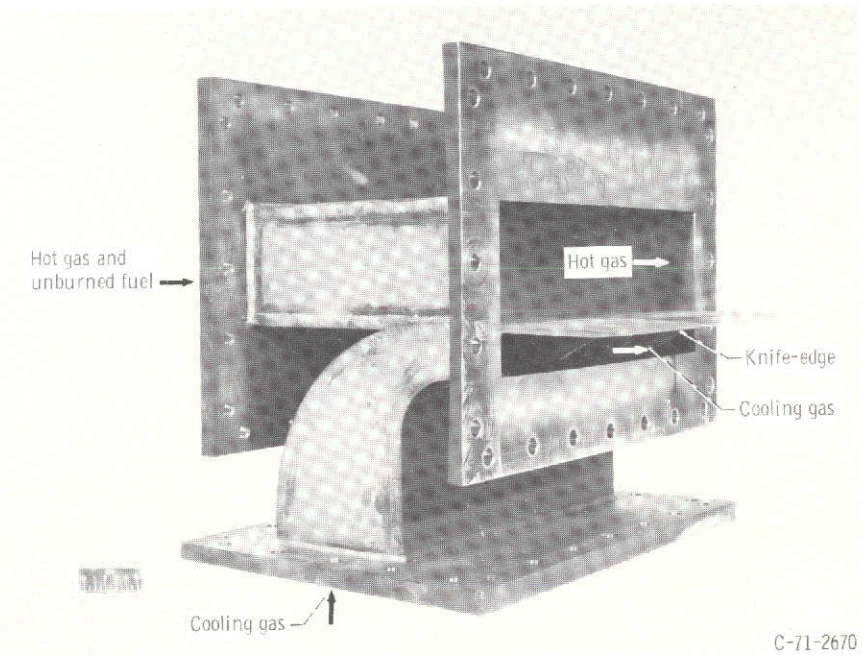

(a) Knife-edge section.

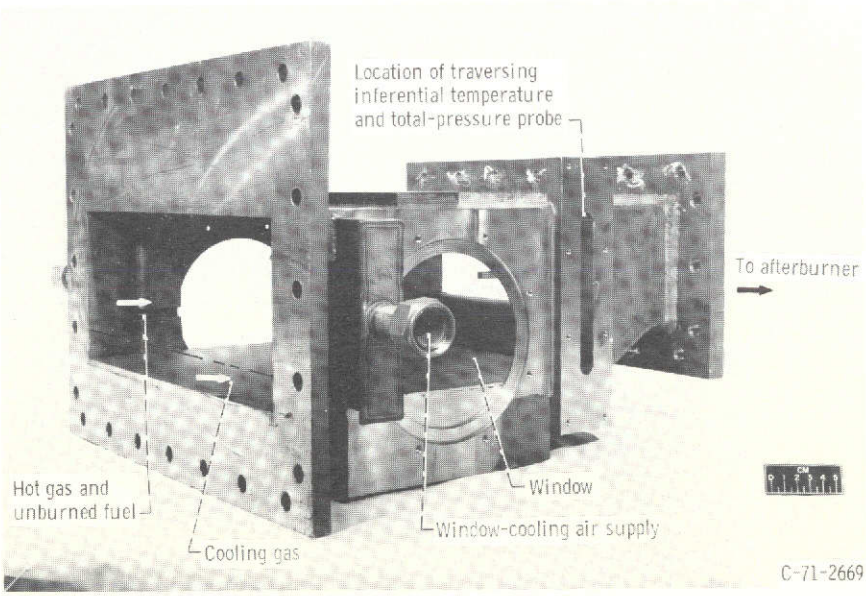

(b) Test-plate section without test plate in place.

Figure 4. - Test section.

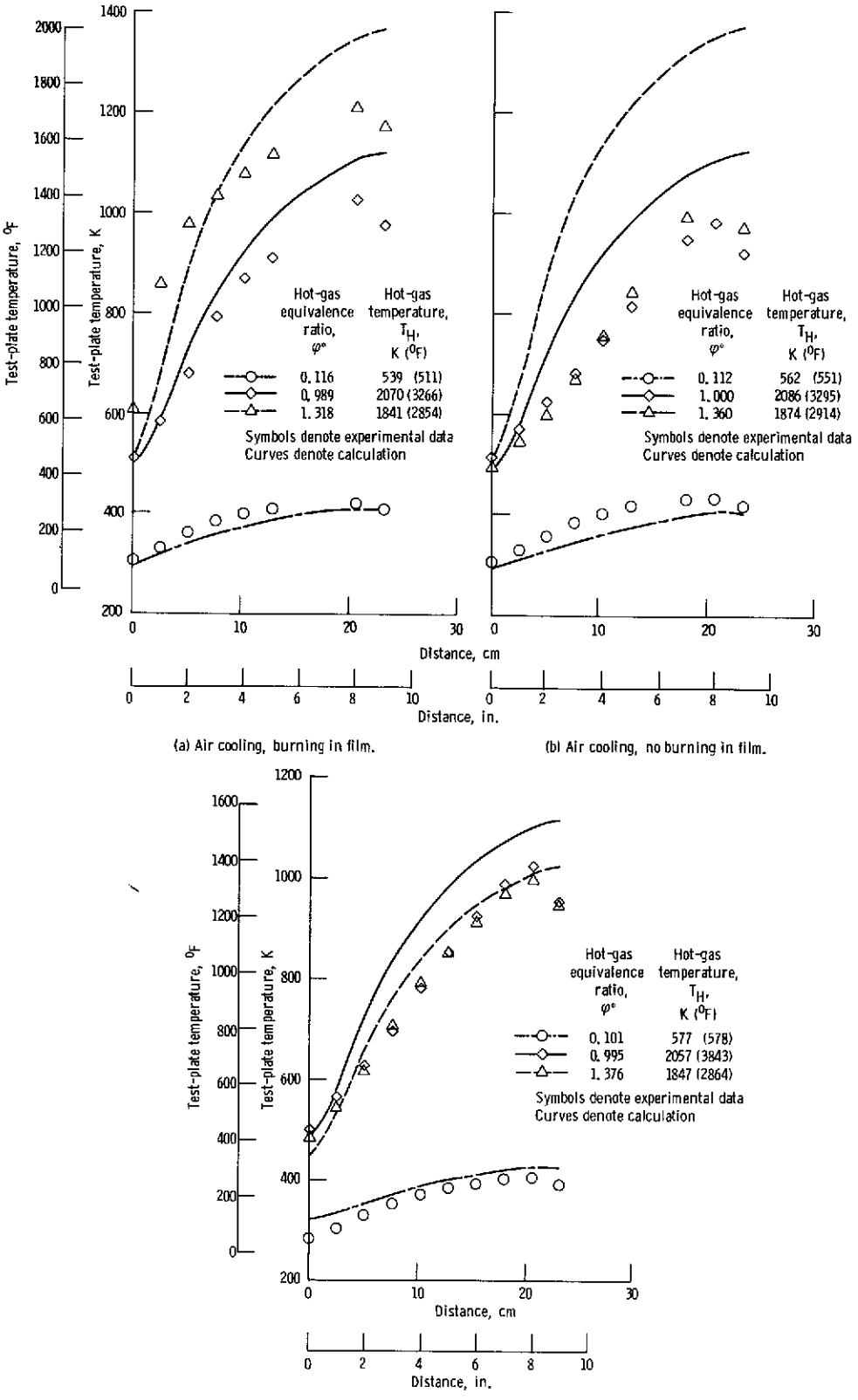

Figure 5. - Test-plate temperature as function of axial distance from knife-edge. Cooling-gas flow rate, 9.5 percent of total flow; mass-flux ratio, $\rho_s u_s / \rho_H u_H = 1.7$; pressure, 1 atmosphere.

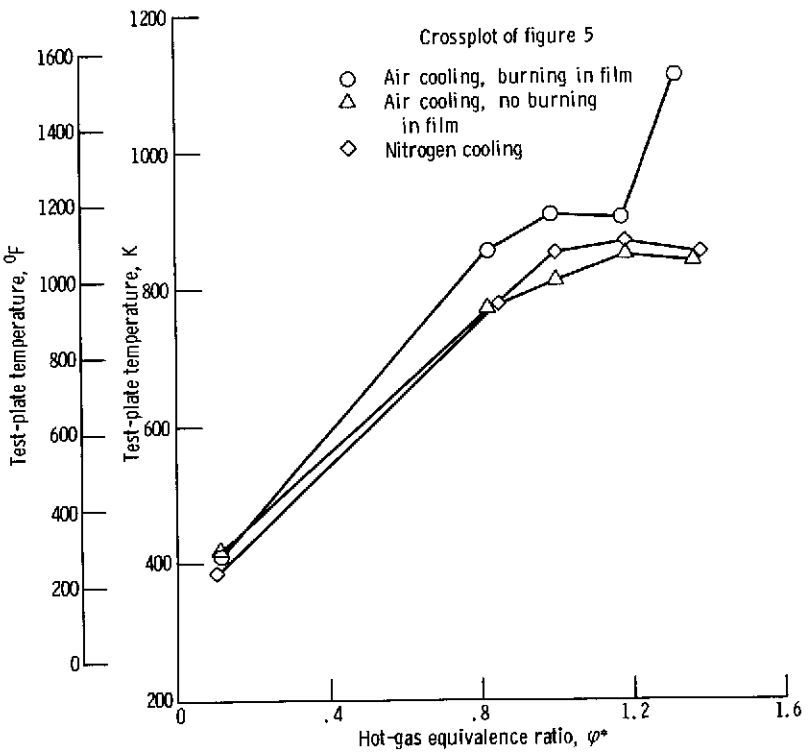

Figure 6. - Test-plate temperature at 12.7 centimeters (5 in.) from the knife-edge as function of equivalence ratio. Cooling-gas flow rate, 9.5 percent of total flow; mass-flux ratio, $\rho_S u_S / \rho_H u_H = 1.7$; pressure, 1 atmosphere.

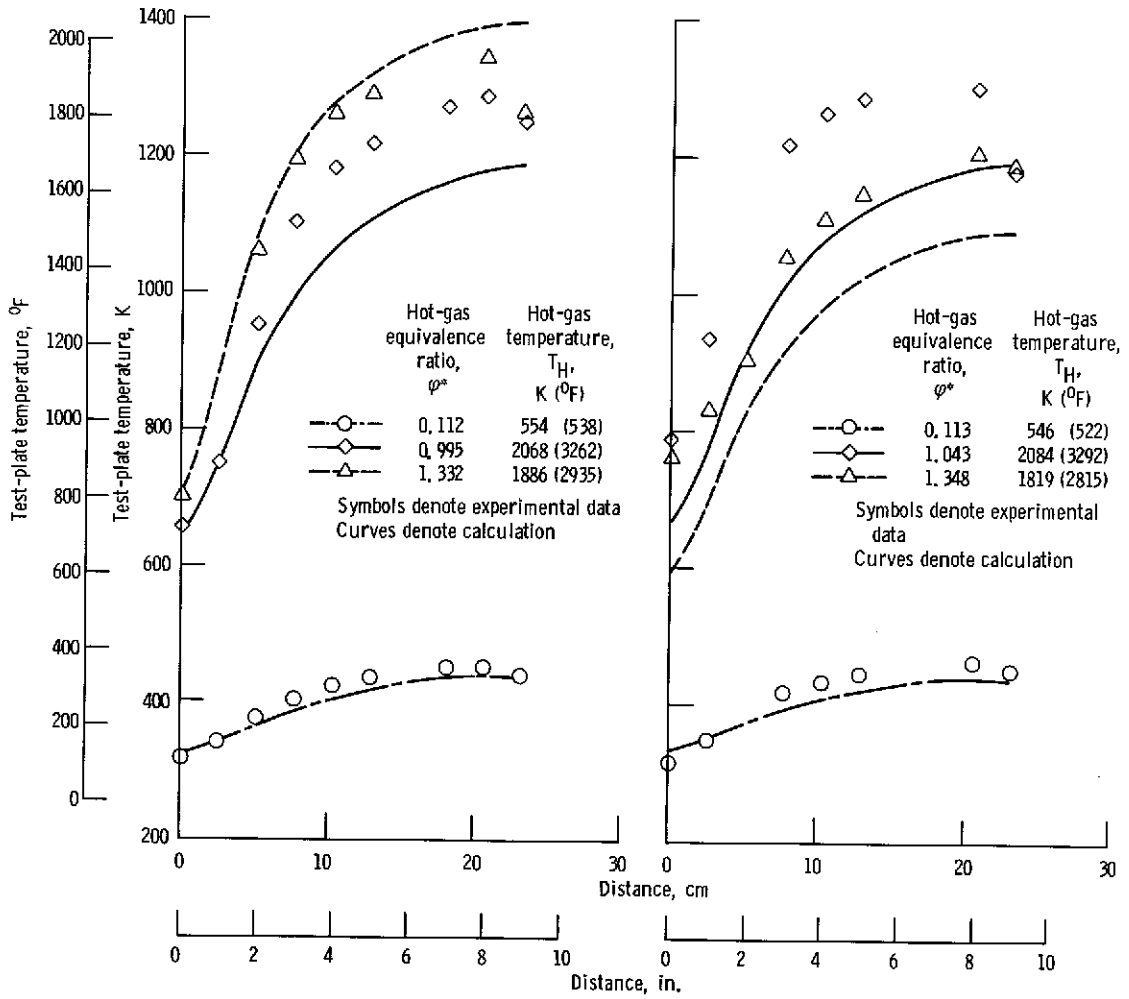

(a) Air cooling.

(b) Nitrogen cooling.

Figure 7. - Test-plate temperature as function of axial distance from knife-edge. Cooling-gas flow rate, 5 percent of total flow; $\rho_S u_S / \rho_H u_H = 0.9$; pressure, 1 atmosphere.

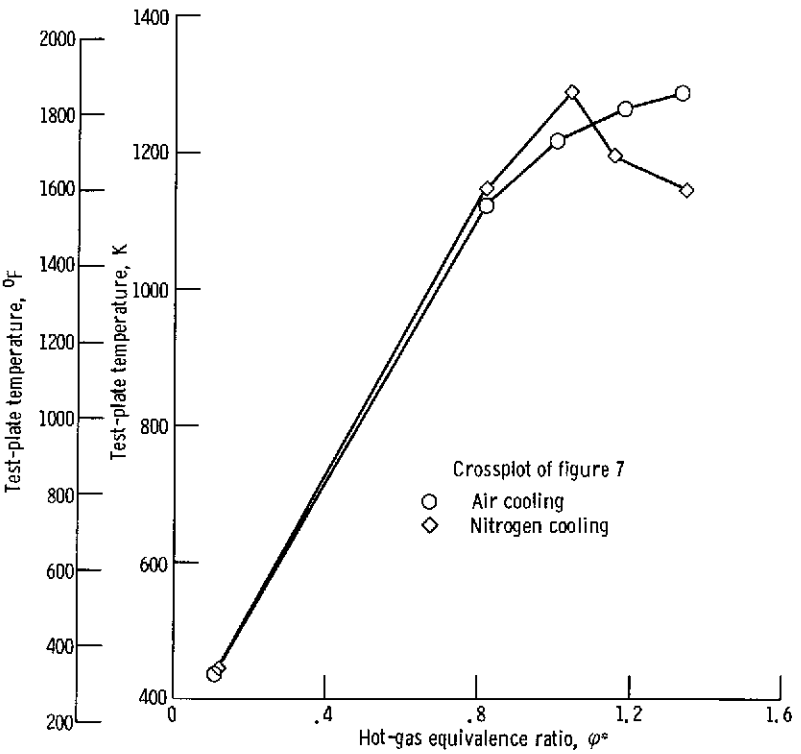

Figure 8. - Test-plate temperature at 12.7 centimeters (5 in.) from the knife-edge as function of equivalence ratio. Cooling-gas flow rate, 5 percent of total flow; mass-flux ratio, $\rho_s u_s / \rho_H u_H = 0.9$; pressure, 1 atmosphere.

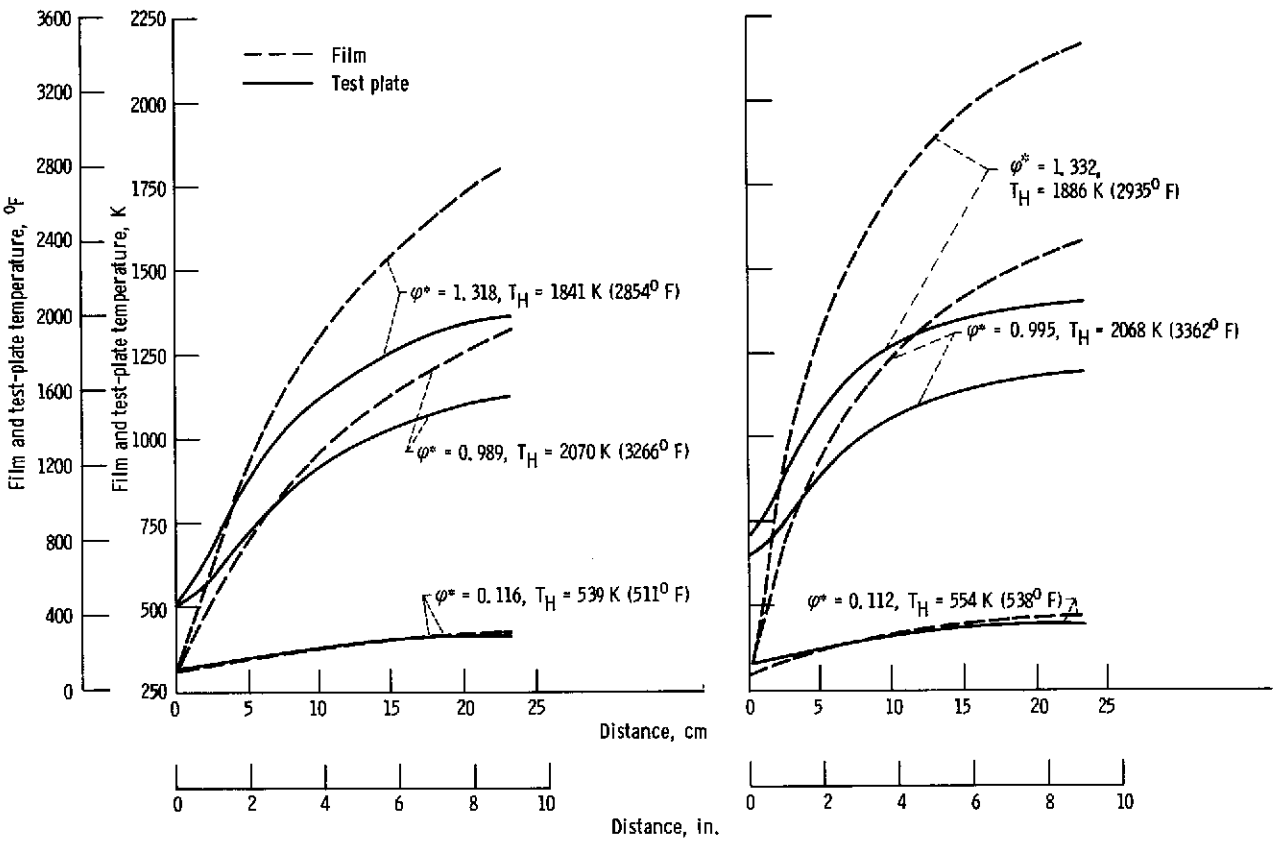

(a) Cooling-gas flow rate, 9.5 percent of total flow.

(b) Cooling flow rate, 5 percent of total flow.

Figure 9. - Comparison of calculated film temperature and calculated test-plate temperature with air cooling.

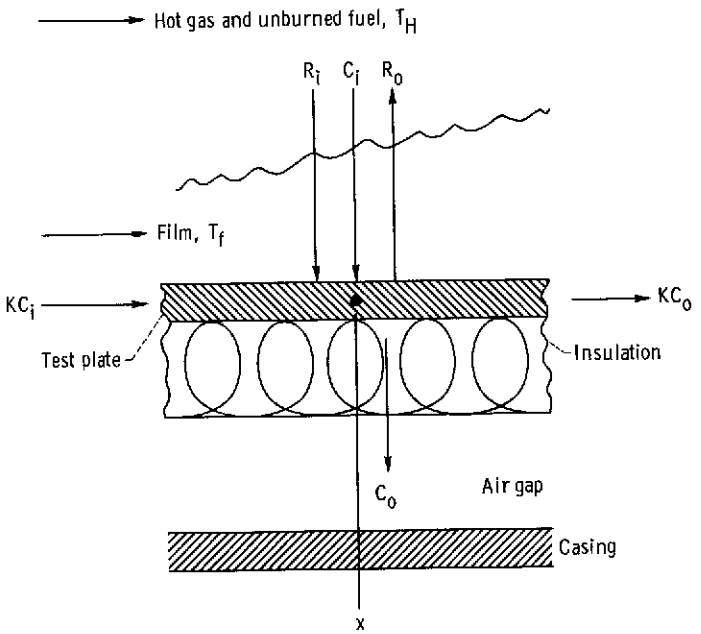

Figure 10. - Sketch showing heat-flux terms.

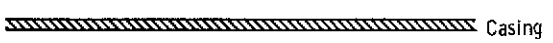

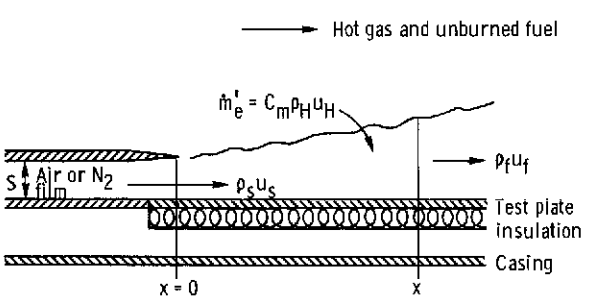

Figure 11. - Sketch of model used in analysis.

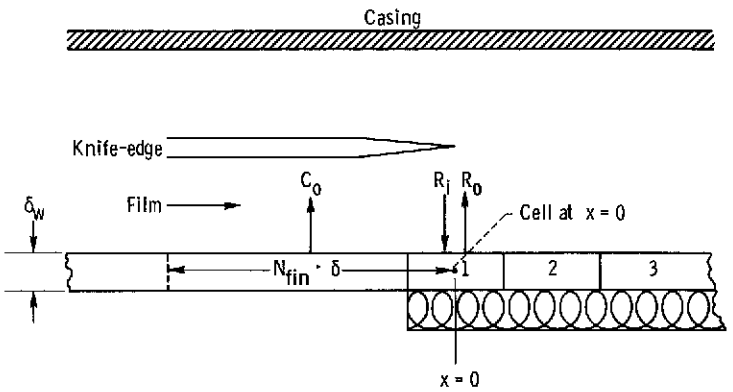

(a) Boundary conditions at knife-edge.

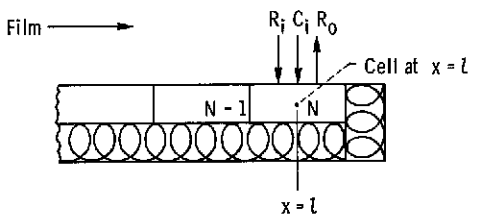

(b) Boundary conditions at end of test plate.

Figure 12. - Boundary conditions.

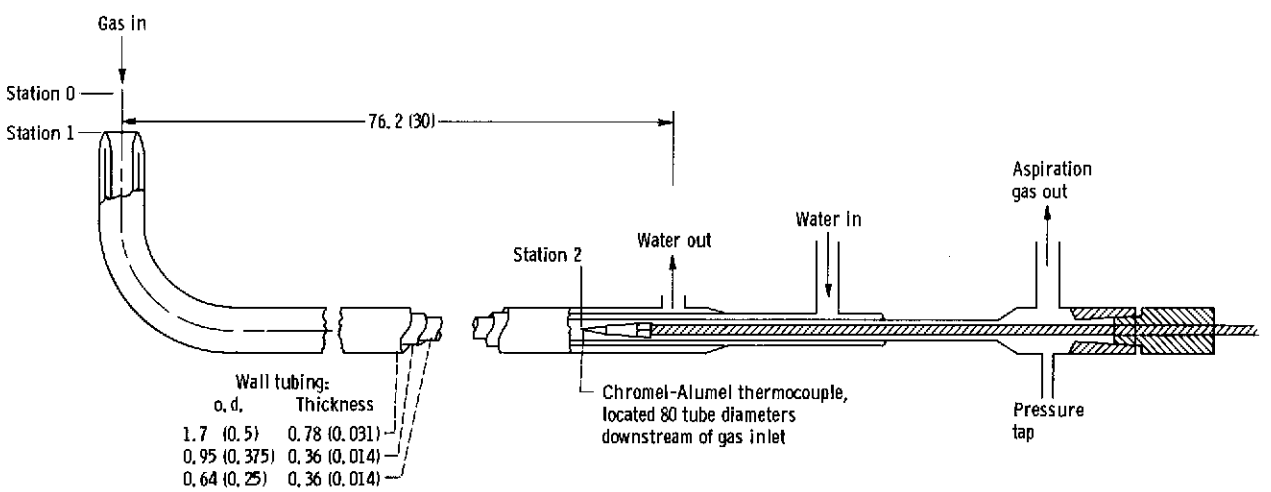

Figure 13. - Schematic of cooled-gas pyrometer. Dimensions are in centimeters (in.).

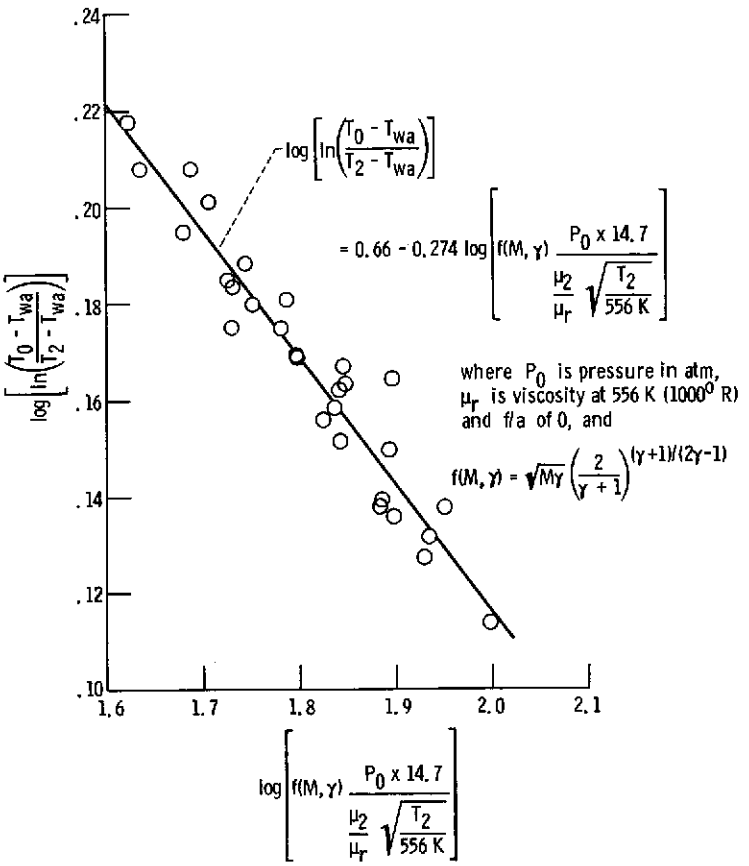

Figure 14. - Calibration plot of cooled-gas pyrometer.